



Comparison between in-mould and grid-as-mould aluminum foaming process by induction heating

Antonio Formisano¹ · Massimo Durante¹ · Francesco Galise²

Received: 5 September 2022 / Accepted: 25 January 2023 / Published online: 2 February 2023
© The Author(s) 2023

Abstract

In the last decades, metal foams have been bringing increasing attention because they represent a new category of materials with very intriguing physical and mechanical properties like, for example, high stiffness and low density. These materials have not been studied completely, and many research efforts have been carrying out to investigate new foaming techniques. The present work aimed at evaluating the efficiency of electromagnetic induction as a heating technique of foam precursors for the manufacture of closed-cell aluminum foam specimens by the indirect foaming process known as the powder compact melting technique; a conventional and a flexible mold strategy, the latter using a stainless-steel wire mesh, were employed for the manufacture of parallelepiped specimens. The results outlined the interesting perspectives of this manufacturing method. In detail, they highlighted a significant process repeatability and the beneficial effects of the induction heating method, allowing heating the precursor in very little time and in a safe way compared to conventional heating through a muffle furnace; moreover, they showed the influence of the mould choice both on the processing time, with the synergistic interaction between the flexible mold and the induction system in terms of heat generation, and on the surface geometry of the foamed components, which reflected in their different compression behavior.

Keywords Aluminum foam · Powder compact melting · Induction heating · Compression tests · Foaming time

1 Introduction

Solid metal foams with closed, partially open, or open cells have been attracting significant interest both from a scientific viewpoint and the prospect of industrial applications; they present a combination of physical and mechanical characteristics that make them very attractive in both structural and functional engineering applications [1]. Concerning the last ones, metal foams can be used as cores of lightweight constructions like structural sandwich panels, ensuring high

stiffness and low weight; furthermore, they support large deformations under almost constant stress and, in so doing, guarantee high energy absorption [2]. Different metals and metal alloys can be considered to produce metal foams, and closed-cell aluminum alloy foams are among the most popular; they are isotropic highly porous metal foams, whose essentially spherical and closed pores occupy about 70% of their volume.

Various foaming methods have been developed; they can be distinguished into two groups, namely, direct and indirect foaming [3]. Direct foaming necessitates a specially prepared molten metal, in which non-metallic particles are dispersed uniformly; the bubbles are obtained by adding gas. This operation is done, among others, through a capillary or porous frit, by using a gas dissolved in the metal which is precipitated into bubbles by temperature or pressure control or by adding a chemical agent which decomposes in the melt. Indirect foaming involves the melting of a solid precursor, consisting of a metallic matrix in which blowing agent particles (generally titanium or zirconium hydride when considering aluminum-based alloys) are uniformly

✉ Antonio Formisano
aformisa@unina.it

Massimo Durante
mdurante@unina.it

Francesco Galise
francesco.galise@crf.it

¹ Department of Chemical, Materials and Production Engineering, University of Naples Federico II, P.Le V. Tecchio 80, 80125 Naples, Italy

² Centro Ricerche Fiat, Composite Materials, Via Ex Aeroporto, 80138 Pomigliano D'Arco (Na), Italy

dispersed. When the matrix melts, the precursor expands and assumes the foam configuration [4].

A very common indirect foaming process is known as the powder compact melting (PCM) technique: It provides the production of foam starting from a dense semi-finished precursor, obtained by compacting a mix of metal powders and a powdered blowing agent; in this technique, accurate preparation of the precursor is of crucial importance to guarantee a good foamability, in terms of density distribution after foaming and repeatability of the foaming process [5].

Several authors' works were concerned with PCM. In detail, a commercial aluminum alloy precursor was used for the production of aluminum foam-based sandwich structures, whose bending [6] and compression behavior [7] were evaluated. Moreover, in another work, the authors developed an innovative single-step process based on the PCM technique, to manufacture structures with a core of aluminum foam and a steel welded wire mesh as reinforcement and, also, as a flexible mould (grid-as-mould process) [8]. It is worth highlighting that the use of a steel wire mesh does not represent a complete novelty in aluminum foam processes. Indeed, it was used to improve the behavior under quasi-static loads of cylindrical [9] and parallelepiped sandwich structures [10], obtained by a traditional in-mould process. Furthermore, the effectiveness of using a steel mesh as mould for the foaming by optical heating of complex shaped parts was proven by Hangai et al. [11], but they did not consider it as a foam reinforcement.

The authors' experimentations described above involved the use of an electric muffle furnace as a heater; but this heating method can determine non-uniform temperature distribution, as well as high process times (preheating plus foaming); in addition, you may run into safety issue during the insertion/extraction operations of the foamed products. So, different heating methods can be considered, to guarantee short times, as well as process monitoring and control. For example, laser heating presents some interesting characteristics: In this method, a laser beam is irradiated with a specific velocity along a desirable path. However, laser energy can be partially dissipated into the cold substrates due to heat conduction; consequently, its main applications are in coating and repair operations [12].

Conversely, induction heating (IH) is a fast, precise, and repeatable non-contact heating method, efficient for metals or other electrically conductive materials in several industrial applications [13].

Its success comes from the fact that the heating source is directly generated inside the body to be heated and, consequently, guarantees higher control and localization, compared to processes using external heating sources [14]; IH can be designed as an intrinsically safe process, since there is no external heat source that requires special safety precautions. In addition, an induction heater can be coupled to a

programmable machine (e.g., a robot or a CNC machine) to heat desired areas of workpieces accurately [12].

Two methods of heating are considered when using this technology, i.e., Joule heating, due to the eddy currents, and hysteretic heating, due to the energy generated by the alternating magnetic field. Consequently, a comprehensive understanding of the IH involves the knowledge of several laws and phenomena like, among others, the Faraday's law, the Maxwell's equations, the Fourier's law, the Ohm's law, the Joule-Lenz's law, the skin effect, and the proximity effect.

The processes using IH involve both low and very high temperatures, with brief (fractions of a second) or very long (months) heating times. Among the most popular applications of IH, consider domestic and commercial cooking, but at the same time industrial cases, as well as research and development. For example, IH is strongly used for joining processes: brazing of dissimilar metals [15]; pre-heating for laser welding of steel joints [16]; melting of thermoplastic adhesives for CFRP materials [17]. Moreover, IH can be used as a heating method for the manufacture of copper-based sintered composites [18]. Finally, the feasibility of this energy source has been recently explored for the additive manufacturing of metallic parts [19]. Concerning the induction heater, it includes an induction power supply that converts line power to an alternating current and powers an inductor (made of a material with high thermal conductivity and low electrical resistivity, generally copper), creating an electromagnetic field that depends on the dimensions and the shape of the inductor.

The IH solution has been already used to produce aluminum foams. For example, it was considered in the foaming process of aluminum by complex stirring, highlighting very good temperature control [20]. Moreover, a preliminary authors' work using IH [21] was carried out by varying the voltage, the resonance frequency (through two different coil inductors), and the configuration (relative position between the specimens and the inductors). The tests highlighted the ability to heat the precursors employing induction in a few seconds, unlike what required through a muffle furnace; in addition, when using the grid-as-mould process, the box of mesh acted as a mould, with the moulded material that did not come out of it [8]. Moreover, the heating was more efficient when the precursor was placed inside the inductor (even if this determines a limit tied to the geometrical limits imposed by the internal dimensions of the coil) [22]. Finally, the lower resonance frequency allowed more controlled and uniform heating, due to a slower heating rate and a higher penetration depth [23].

Based on these previous results, the present work is meant to represent research useful to lay the basis for investigating the PCM method combined with electromagnetic induction; it showed its suitability and efficiency, and compared

the manufacturing of aluminum foams components by the traditional in-mould and the innovative grid-as-mould process, in terms of process fastness and mechanical properties. In detail, a commercial foamable-solid precursor and a stainless-steel wire mesh were employed to carry out both in-mould and grid-as-mould foaming processes, by varying the voltage of the IH system and using one only inductor and configuration (relative specimens/inductor positioning); a comparison between the products from the two foaming processes, in terms of foaming times and the compression behavior, was carried out. The results of the experimental campaign highlighted a significant process reproducibility, as well as the high efficiency of the induction heating method, particularly when considering the single-step strategy based on the grid-as-mould flexible solution; moreover, they also showed the influence of the moulding strategy on the geometrical and mechanical characteristics of the specimens. This suggests a wide potential for IH-based foaming processes based on the PCM method and points the way towards developing new systems to produce complex foam parts.

2 Materials and methods

An EGMA 30R inductive heating generator, designed by Felmi, was used for the experimental campaign; it grants reliability, safety, and repeatability to the heating process. The generator presents a maximum power of 30 kW, while the voltage can be tuned, up to a maximum of about 500 V; the chilling is through water flow.

The generator presents an automatic “hooking system” of the resonance frequency, called auto-tuning system, which

allows using inductors with different induction values without any need of resetting or recalibrating the device. It can control the frequency of oscillation of the current, equal to the following:

$$f = \frac{1}{2\pi\sqrt{LC}} \quad (1)$$

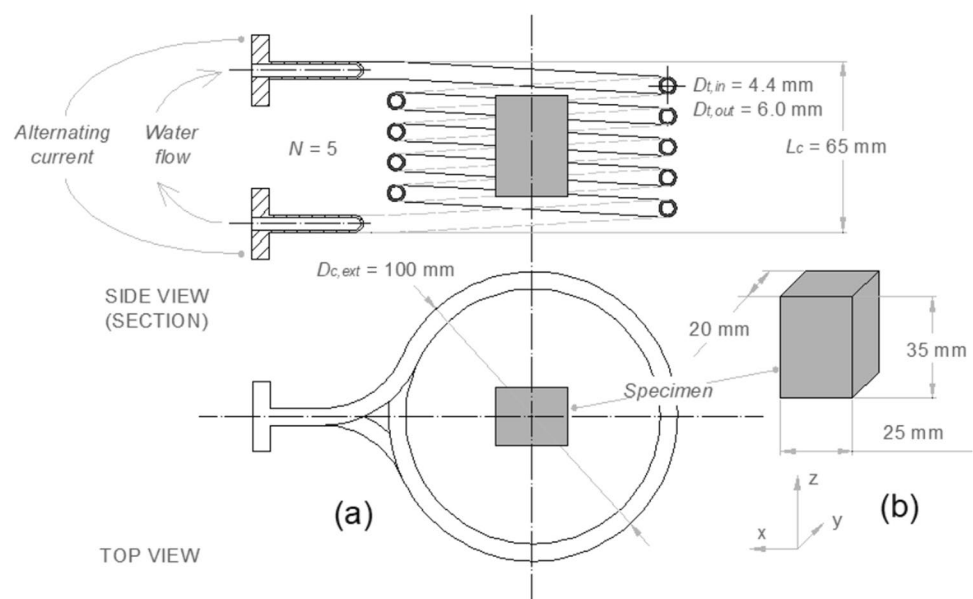
where C is the capacitance of the system and L is the inductance of the inductor.

The inductor was a coil, obtained by an annealed copper tube (filled with a water flow for its cooling) with inside and outside diameters $D_{t,in} = 4.4$ mm and $D_{t,out} = 6.0$ mm, respectively; the coil had an external diameter $D_{c,ext} = 100$ mm, $N = 5$ turns, and a total length $L_c = 65$ mm. The actual resonance frequency, monitored by the control panel of the system, was $f = 70$ kHz. This inductor, together with the choice to place the specimens into it, represented the best solution for controlled and uniform heating [21]. A schematic illustration of the inductor (a) and a specimen (b) is reported in Fig. 1.

The control panel also monitored the other operating parameters, like the power, the current, and the voltage; five voltage levels (labelled from V1 to V5) equal to 218, 309, 378, 436, and 488 V were tested.

The aluminum foam precursor was a commercial Alulight AlSi 10 TiH₂-0.8 product [24], which is a mixture of Al, Si (10 wt%) and TiH₂ (foaming agent; 0.8 wt%) powders, in the form of extruded strips with a cross-section of 20 mm × 5 mm and a density of 2.5 g/cm³. An elastoplastic with isotropic hardening 0/90 stainless-steel welded wire mesh was used as a flexible mould; it is constituted by wires with a diameter of 0.8 mm and a 6 mm × 6 mm grid. This type of wire mesh

Fig. 1 Schematic illustration of the inductor (a) and a specimen (b)



proved to be efficient both as flexible mould and as reinforcement under bending load, showing flexibility and capability of holding the molten foam, and allowing a mechanical joining with the solid foam [8]. The main characteristics of the precursor and the wire mesh are reported in [9].

Preliminary free foaming tests were carried out, placing pieces of precursor (18 g in mass) into commercial truncated cone-shaped ceramic crucibles with a diameter at its mid-height of about 40 mm, to evaluate the density and observe the morphology of the foam when the precursor was free to expand; these features were compared to the corresponding ones in the literature, to evaluate the goodness of the foaming process by IH.

Considering the results of the preliminary tests, in-mould (self-made, with refractory materials) and grid-as-mould tests were carried out to obtain parallelepiped specimens (at least three in number), whose dimensions are reported in Fig. 1; the tests were conducted by varying the voltage. Figure 2 reports pieces of foam precursor (a) and a grid-as-mould specimen (b) before foaming. For all the cases (in-crucibles, in-mould, and grid-as-mould foaming tests), supports were used to place the specimens in the central zone of the inductor; Fig. 3 reports the setup of an in-mould foaming test. Moreover, the cooling of the specimens after foaming was in the air.

The two foaming processes were compared in terms of foaming times and compression behavior; uniaxial compression tests were carried out by pressing the specimens along the z -axis (in-mould- z and grid-as-mould- z specimens) and the y -axis of Fig. 1b (in-mould- y and

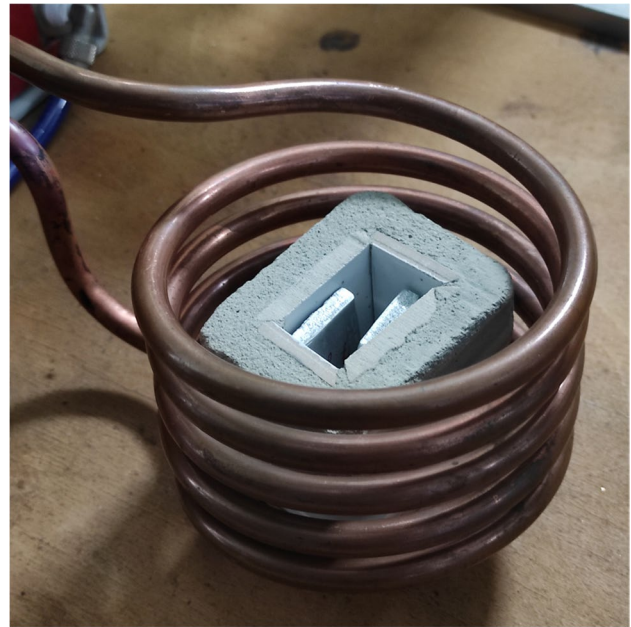
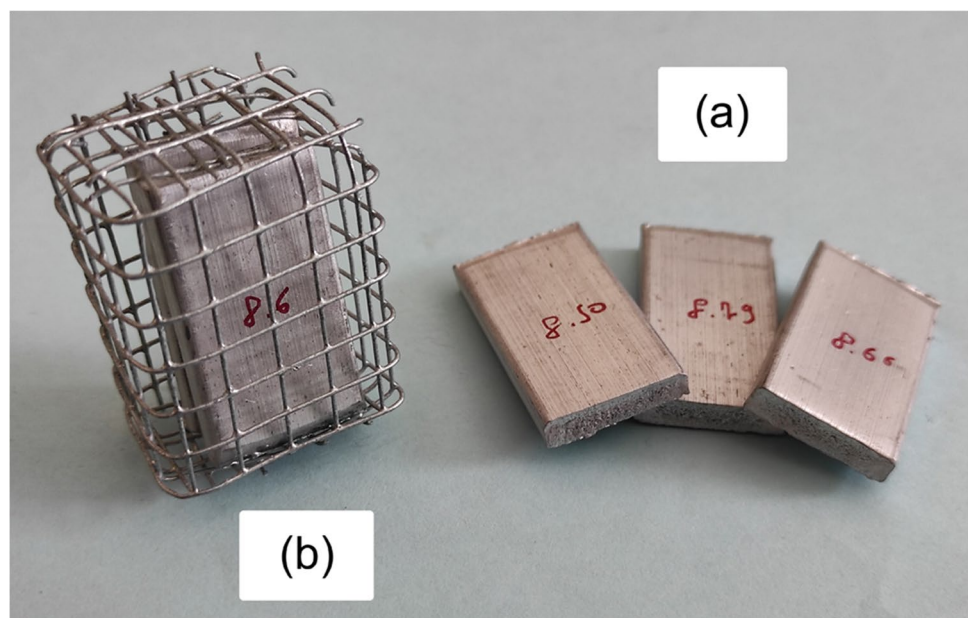


Fig. 3 Setup of the in-mould process

grid-as-mould- y specimens), using an MTS Alliance RT/50 testing machine equipped with a 50 kN load cell, at a speed of 2 mm/min. Given the surface irregularities of the specimens, their cross-section areas for the evaluation of the stresses were measured with the support of a CAD software. Three specimens were tested for each type of sample to ensure statistically significant results.

Fig. 2 Pieces of foam precursor (a) and a grid-as-mould specimen (b) before foaming



3 Results and discussion

The preliminary free foaming tests were carried out at the V5 voltage level; the foaming time was equal to 35 s. Figure 4 reports the section of a specimen from this preliminary campaign; the cut was conducted by a metallographic cut-off saw at its mid-height. From the figure, a typical structure of closed-cell aluminum foams was observed, with the distribution and combination of the cell units characterized by randomness and irregularity of the pores (in terms of shape and dimensions) [25]; the maximum pore size did not exceed about 4 mm, with the major part of this feature not exceeding 2 mm. The density was equal

to 0.72 g/cm^3 , corresponding to a relative density of 0.29; this value falls in the range of 0.1–0.3, typical of Alulight commercial foams [26]. Given the morphological characteristics and the density of the foams, the preliminary tests highlighted the efficiency of induction as a heating method for foaming processes.

After the preliminary tests, the parallelepiped specimens for the mechanical characterization were manufactured. To obtain a similar density (see Fig. 1b) and considering cutting operations (which eliminate the densified parts), two pieces of the precursor of about 8 g each were used for both in-mould and grid-as-mould processes; the in-mould process was carried out leaving open the upper part of the mould, to control the foaming (see Fig. 3).

Figure 5 shows some specimens obtained by the in-mould (a) and grid-as-mould (b) process when setting the V3 voltage level, while the graph in Fig. 6 reports the average foaming time depending on the level of voltage; it is

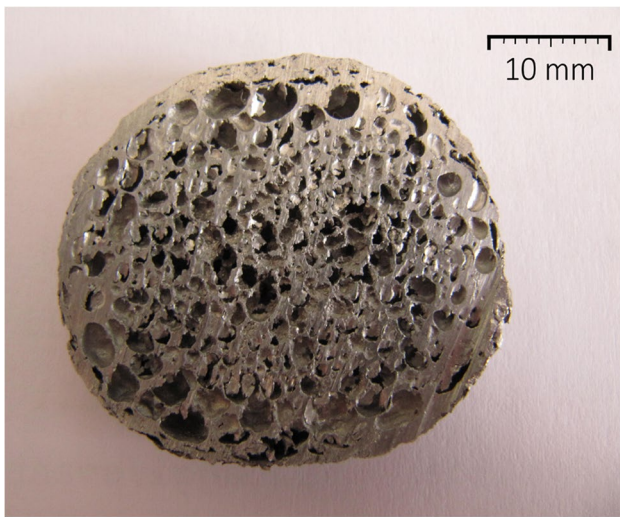


Fig. 4 Section of a specimen obtained in a truncated cone-shaped crucible

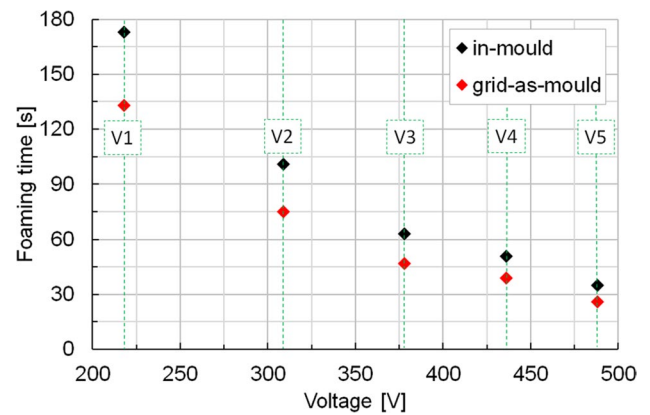


Fig. 6 Foaming time as a function of the voltage

Fig. 5 In-mould (a) and grid-as-mould (b) specimens



worth reporting a non-significant variability of this feature at setup parity (the foaming times differed by less than 1 s), highlighting very good repeatability of the foaming process.

Figure 5 shows that the moulding strategy influenced the foam geometry; the in-mould specimens (Fig. 5a) reproduced quite closely the designed shape, excluding the upper surface for the absence of the corresponding part of the mould. Concerning the grid-as-mould specimens (Fig. 5b), the grid acted as a mould; in fact, the moulded material penetrated and did not come out of it, and assuming a rounded shape at the end of the solidification. Therefore, the external surface of the specimens did not perfectly reproduce the designed shape. In addition, no interfacial reaction occurred between the grid and the foam because of oxidation phenomena [27]; consequently, a mechanical joining only took place between them [8].

Figure 6 confirms that IH was a fast method, due to its localized nature. This allowed foaming times never higher than 173 s, recorded for an in-mould process at the lowest voltage level (V1). For comparison purposes, consider that a correct foaming of the samples described in [8, 9], using a 3 kW muffle furnace, was obtained in a time ranging between 12 and 15 min, while the preheating time (from room temperature to a foaming temperature of about 660 °C) was of about 77 min. Moreover, the foaming time decreased almost linearly with the voltage for both process strategies. Finally, the grid-as-mould process represented the fastest solution; the time reduction, t_R (see Eq. 2) fell in the range of 30 ÷ 35%:

$$t_R = \frac{t_{in-mould} - t_{grid-as-mould}}{t_{grid-as-mould}} \cdot 100 \quad (2)$$

where $t_{in-mould}$ and $t_{grid-as-mould}$ represent the foaming times for the in-mould and grid-as-mould processes. This behavior was justified by the synergistic effect of the grid, which interacted with the inductor and increased the heat generation, so as highlighted in Fig. 7.

After these considerations on the feasibility of the process, the compression behavior of specimens from the two samples was evaluated. To this end, flat faces were obtained by cutting the upper and lower parts of the specimens; after these trimming operations, the density was equal to 0.73 and 0.69 g/cm³ for, respectively, the in-mould and grid-as-mould specimens. As mentioned above, the tests were carried out along two directions; by doing so, it was possible to evaluate the influence of the walls (and, eventually, of the grid) on the compression behavior of the foams for two extreme cases: four (z-direction) and two smallest lateral walls (y-direction).

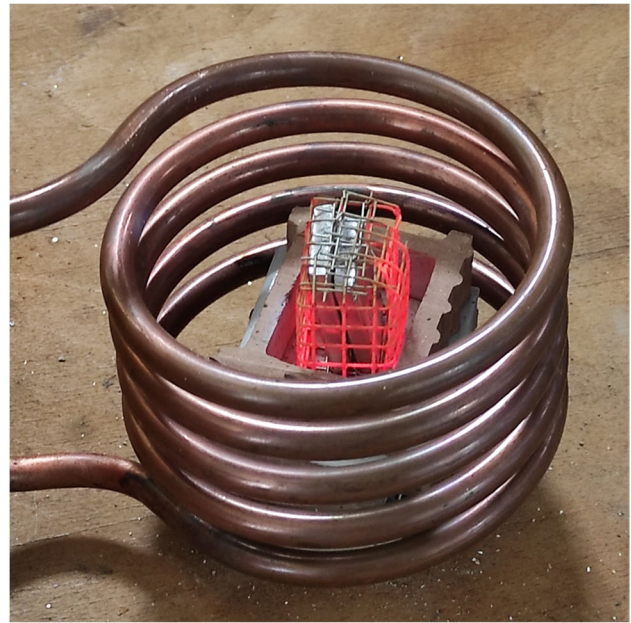


Fig. 7 Execution of a grid-as-mould process

The compression tests were characterized by significant repeatability of the results at mould strategy and compression direction parity; the voltage of the induction system did not influence the mechanical behavior. Figures 8 and 9 report examples of them for all the typologies and the corresponding stress–strain curves. From Fig. 9, you can note that the $_z$ specimens exhibited higher strength and stiffness (similar for the two mould strategies, see the first almost linear region of the curves), compared to the corresponding $_y$ ones; this can be attributable to the influence of the walls, which acted as reinforcements, particularly for the $_z$ specimens. Moreover, the curve that best showed the typical shape of metallic foam [28] was the grid-as-mould $_z$ one. In detail, it presented a first region (up to about 1% of strain) characterized by elastoplastic deformation due to partially reversible cell walls bending, followed by a plateau up to 45% of strain and determined by buckling, yielding and fracture of the cell walls and, finally, a rapid stress increase, due to the foam compaction [29]. Conversely, the in-mould specimens showed an increasing trend just after the first region (corresponding to a strain of about 5% and stress of about 17 and 8 MPa for the $_z$ and the $_y$ specimens, respectively); this was due to the densification of the molten foam when came into contact with the mould walls, which creating a more resistant skin around the specimens, while this effect did not occur for the grid-as-mould specimens, less constrained along the external surface by the flexible and partially open mould. Finally,

Fig. 8 Compression tests on in-mould_z (a), grid-as-mould_z (b), in-mould_y (c), and grid-as-mould_y (d) specimens

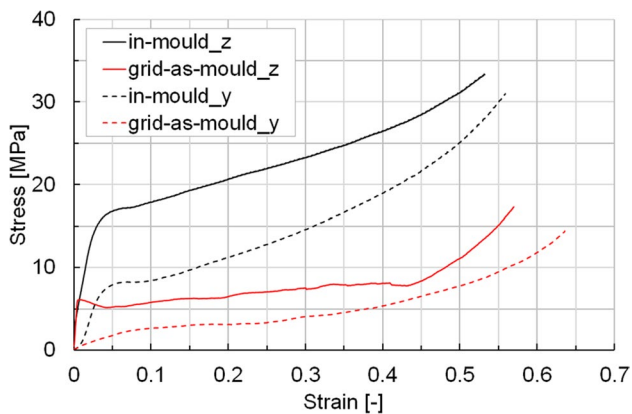
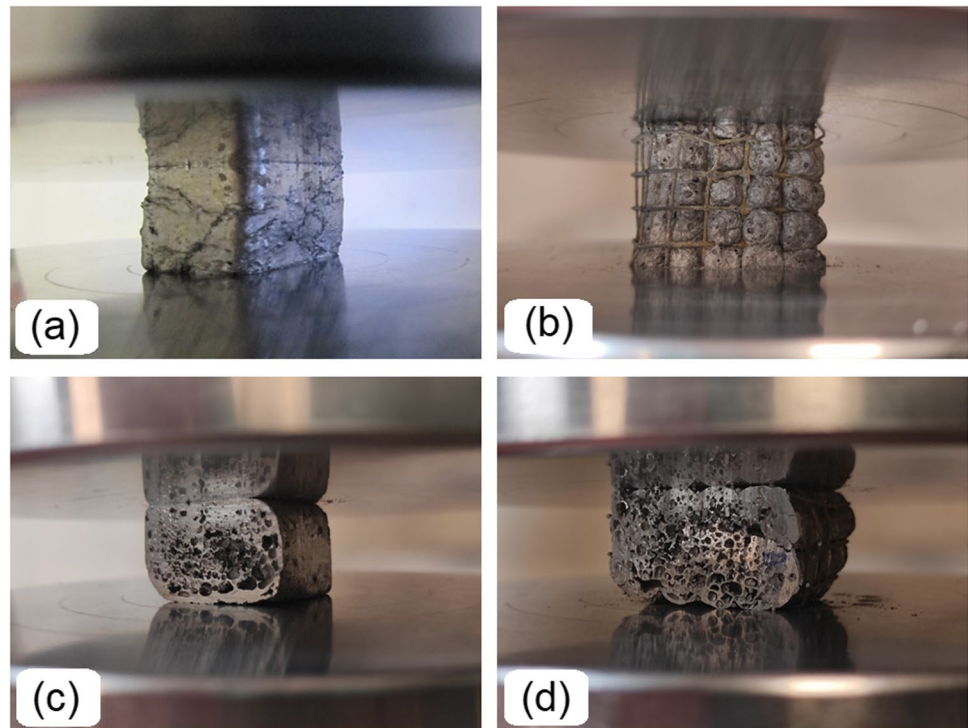


Fig. 9 Stress–strain curves from compression tests

for the grid-as-mould process, the grid seemed not to act as a reinforcement under compression as efficiently as observed under bending [8], due to the tendency to buckle of the wire mesh when subject to compression loads. The plateau stress for grid-as-mould_z and the grid-as-mould_y was equal to, respectively, about 6 and 3 MPa; considering that the foam of these specimens presented a density of 0.43 g/cm^3 (the evaluation was made by excluding the contribution of the wire mesh in terms of mass and volume), the plateau stresses were similar to the ones of Alulight panels with equal density, showing a value of about 3.5 MPa [30].

4 Conclusions

The work highlighted that electromagnetic induction was an efficient and fast heating technique to foam aluminum precursors by the powder compact melting method; this statement was also valid for a conventional in-mould process and an innovative variant, which involved the use of a stainless-steel wire mesh as a flexible mould. The localized nature of the heating systems allowed the foaming of parallelepiped specimens in very little time (26 s when using the grid-as-mould solution and a voltage of about 500 V, with a time reduction of about 35% compared to the in-mould method, thanks to the synergistic effect of the grid). The compression behavior and the surface geometry were strongly influenced by the mould type, and the in-mould process generated nearly as designed and more resistant specimens, due to a most significant skin effect because of the foam densification. Finally, the repeatability of the results in terms of foaming time and stress–strain curves suggested high control of the induction heated-based foaming process.

Future works could involve the optimization of the process: For example, FEM analyses could be considered to better understand some aspects, like the heat field propagation depending on the main features of the magnetic field. Moreover, ad hoc inductors could be designed, as well as the relative specimen/inductor positioning optimized; in doing so, an induction heating-based system could be developed along the lines of continuous metal additive processes for the

manufacturing of complex freeform foam components for industrial applications and of suitable specimens for a deepen mechanical and morphological characterization.

Author contribution All authors contributed to the study, conception and design. Material preparation was performed by Antonio Formisano and Massimo Durante; the tests were carried out by Antonio Formisano and Francesco Galise; and the data analysis was performed by all authors. The first draft of the manuscript was written by Antonio Formisano, and all authors commented on previous versions of the manuscript. All authors read and approved the final manuscript.

Funding Open access funding provided by Università degli Studi di Napoli Federico II within the CRUI-CARE Agreement.

Data availability The associated data and material will not be deposited. However, the raw/processed data required to reproduce these findings can be available on request to the corresponding author.

Code availability Not applicable.

Declarations

Ethics approval Not applicable.

Consent to participate All authors consent to their participation in the research of this manuscript.

Consent to publication All authors consent to publish the research content of this paper.

Competing interests The authors declare no competing interests.

Open Access This article is licensed under a Creative Commons Attribution 4.0 International License, which permits use, sharing, adaptation, distribution and reproduction in any medium or format, as long as you give appropriate credit to the original author(s) and the source, provide a link to the Creative Commons licence, and indicate if changes were made. The images or other third party material in this article are included in the article's Creative Commons licence, unless indicated otherwise in a credit line to the material. If material is not included in the article's Creative Commons licence and your intended use is not permitted by statutory regulation or exceeds the permitted use, you will need to obtain permission directly from the copyright holder. To view a copy of this licence, visit <http://creativecommons.org/licenses/by/4.0/>.

References

- García-Moreno F (2016) Commercial applications of metal foams: their properties and production. *Mater* 9:85. <https://doi.org/10.3390/MA9020085>
- Banhart J (2005) Aluminium foams for lighter vehicles. *Int J Veh Des* 37:114–125. <https://doi.org/10.1504/IJVD.2005.006640>
- Banhart J (2013) Light-metal foams—history of innovation and technological challenges. *Adv Eng Mater* 15:82–111. <https://doi.org/10.1002/ADEM.201200217>
- Banhart J (2006) Metal foams: production and stability. *Adv Eng Mater* 8:781–794. <https://doi.org/10.1002/ADEM.200600071>
- Youn SW, Kang CG (2004) Fabrication of foamable precursors by powder compression and induction heating process. *Metall Mater Trans B Process Metall Mater Process Sci* 35:769–776. <https://doi.org/10.1007/s11663-004-0017-5>
- Formisano A, Durante M, Viscusi A, Carrino L (2021) Mechanical behavior and collapse mechanisms of innovative aluminum foam-based sandwich panels under three-point bending. *Int J Adv Manuf Technol* 112:1631–1639. <https://doi.org/10.1007/S00170-020-06564-4>
- Viscusi A, Durante M, Formisano A (2022) An experimental–numerical analysis of innovative aluminum foam-based sandwich constructions under compression loads. *Lect Notes Mech Eng* 131–150. https://doi.org/10.1007/978-3-030-82627-7_8
- Durante M, Formisano A, Viscusi A, Carrino L (2020) An innovative manufacturing method of aluminum foam sandwiches using a mesh-grid reinforcement as mold. *Int J Adv Manuf Technol* 107:3039–3048. <https://doi.org/10.1007/S00170-020-05244-7/FIGURES/9>
- Viscusi A, Carrino L, Durante M, Formisano A (2020) On the bending behaviour and the failure mechanisms of grid-reinforced aluminium foam cylinders by using an experimental/numerical approach. *Int J Adv Manuf Technol* 106:1683–1693. <https://doi.org/10.1007/s00170-019-04414-6>
- An Y, Yang S, Zhao E, Wang Z (2017) Characterization of metal grid-structure reinforced aluminum foam under quasi-static bending loads. *Compos Struct* 178:288–296. <https://doi.org/10.1016/j.compstruct.2017.07.031>
- Hangai Y, Amagai K, Omachi K et al (2018) Forming of aluminum foam using steel mesh as die during foaming of precursor by optical heating. *Opt Laser Technol* 108:496–501. <https://doi.org/10.1016/j.optlastec.2018.07.016>
- Dalae MT, Gloor L, Leinenbach C, Wegener K (2020) Experimental and numerical study of the influence of induction heating process on build rates Induction Heating-assisted laser Direct Metal Deposition (IH-DMD). *Surf Coatings Technol* 384:125275. <https://doi.org/10.1016/j.surfcoat.2019.125275>
- Lucia O, Maussion P, Dede EJ, Burdío JM (2014) Induction heating technology and its applications: past developments, current technology, and future challenges. *IEEE Trans Ind Electron* 61:2509–2520. <https://doi.org/10.1109/TIE.2013.2281162>
- Lupi S, Forzan M, Aliferov A (2015) Induction and direct resistance heating: theory and numerical modeling. *Induction Direct Resist Heat Theory Numer Model* 1–370. <https://doi.org/10.1007/978-3-319-03479-9>
- Demianová K, Sahul M, Behúlová M, Turňa M (2011) Application of high-frequency induction heating for brazing of dissimilar metals. *Adv Mater Res* 214:450–454. <https://doi.org/10.4028/www.scientific.net/AMR.214.450>
- Li L, Mi G, Zhang X et al (2019) The influence of induction pre-heating on microstructure and mechanical properties of S690QL steel joints by laser welding. *Opt Laser Technol* 119:105606. <https://doi.org/10.1016/J.OPTLASTEC.2019.105606>
- Nele L, Palmieri B (2020) Electromagnetic heating for adhesive melting in CFRTP joining: study, analysis, and testing. *Int J Adv Manuf Technol* 106:5317–5331. <https://doi.org/10.1007/s00170-019-04910-9>
- Dewidar MM, Lim J-K (2007) Manufacturing processes and properties of copper—graphite composites produced by high frequency induction heating sintering. *J Compos Mater* 41:2183–2194. <https://doi.org/10.1177/0021998307074145>
- Sharma GK, Pant P, Jain PK et al (2020) On the suitability of induction heating system for metal additive manufacturing. *Int J Adv Manuf Technol* 235:219–229. <https://doi.org/10.1177/0954405420937854>

20. Jeon YP, Kang CG, Lee SM (2009) Effects of cell size on compression and bending strength of aluminum-foamed material by complex stirring in induction heating. *J Mater Process Technol* 209:435–444. <https://doi.org/10.1016/J.JMATPROTEC.2008.02.017>
21. Formisano A, Boccarusso L, Durante M et al (2022) On the suitability of induction heating for the manufacture of reinforced aluminum foam structures. *Key Eng Mater* 926:1689–1695. <https://doi.org/10.4028/P-598BL7>
22. Rudnev V, Loveless D, Cook RL, Black M (2002) *Handbook of induction heating*. CRC Press
23. Moser L (2012) Experimental analysis and modeling of susceptorless induction welding of high performance thermoplastic polymer composites. Dissertation, Institut für Verbundwerkstoffe GmbH, Kaiserslautern
24. Lázaro J, Solórzano E, Rodríguez-Pérez MA et al (2014) Heat treatment of aluminium foam precursors: effects on foam expansion and final cellular structure. *Procedia Mater Sci* 4:287–292. <https://doi.org/10.1016/J.MSPRO.2014.07.559>
25. Lu GY, Su BY, Li ZQ et al (2014) Thermal properties of closed-cell aluminum foam with circular pores. *Therm Sci* 18:1619–1624. <https://doi.org/10.2298/TSCI1405619L>
26. Ashby MF (2000) *Metal foams : a design guide*. Butterworth-Heinemann
27. Luo H, Lin H, Zhao Z et al (2014) Preparation of aluminum foam sandwich reinforced by steel sheets. *Procedia Mater Sci* 4:39–43. <https://doi.org/10.1016/j.mspro.2014.07.589>
28. Banhart J, Baumeister J (1998) Deformation characteristics of metal foams. *J Mater Sci* 33:1431–1440. <https://doi.org/10.1023/A:1004383222228>
29. Koza E, Leonowicz M, Wojciechowski S, Simancik F (2004) Compressive strength of aluminium foams. *Mater Lett* 58:132–135. [https://doi.org/10.1016/S0167-577X\(03\)00430-0](https://doi.org/10.1016/S0167-577X(03)00430-0)
30. Idris MI, Vodenitcharova T, Hoffman M (2009) Mechanical behaviour and energy absorption of closed-cell aluminium foam panels in uniaxial compression. *Mater Sci Eng A* 517:37–45. <https://doi.org/10.1016/J.MSEA.2009.03.067>

Publisher's note Springer Nature remains neutral with regard to jurisdictional claims in published maps and institutional affiliations.